Structural basis of transcription activation by the global regulator Spx

Jing Shi[1,#,*], Fangfang Li[1,#], Aijia Wen[3,4,#], Libing Yu[5,#], Lu Wang[1], Fulin Wang[1], Yuanling Jin[1], Sha Jin[3,4], Yu Feng[3,4,*], Wei Lin[1,2,6,*]

[1] Department of Pathogen Biology, School of Medicine & Holistic Integrative Medicine, Nanjing University of Chinese Medicine, Nanjing, China.

[2] State Key Laboratory of Natural Medicines, China Pharmaceutical University, Nanjing, China

[3] Department of Biophysics, Zhejiang University School of Medicine, Hangzhou, China.

[4] Department of Pathology of Sir Run Run Shaw Hospital, Zhejiang University School of Medicine, Hangzhou, China.

[5] Institute of Materials, China Academy of Engineering Physics, Mianyang, China

[6] Jiangsu Collaborative Innovation Center of Chinese Medicinal Resources Industrialization, Nanjing 210023, China.

#, Equal contribution.

*, Correspondence: weilin@njucm.edu.cn OR yufengjay@zju.edu.cn OR shijing301@njucm.edu.cn

Running title: Structural insights into the physiological function of Spx in bacteria

>t*rxA*-*mango* promoter sequence:

CGGCTGTGATCAGGAAAAAATAATTTGTAAGCATTAAAATAGCGTGAACGAATGGG

AGATGCTATACTAAAAATCATCATTTCACATTGGAGGAATTCAATAATGGCGGCACG

TACGAAGGAAGGATTGGTATGTGGTATATTCGTACGTGCC

>*rrnJ P1*-*mango* promoter sequence:

TAGGGAAAGGATGCCGCTCTTTTTAAATCCCTTAGTATTTCTTCAAAAAAACTATTG

CACTATTATTTACTAGGTGGTATATTATTATTCGTTGCCGCTAAACAAGGCGATAACG

GGCACGTACGAAGGAAGGATTGGTATGTGGTATATTCGTACGTGCC

-44 element UP element -35 element -10 element Transcription products

mango

Figure S1. The sequences of t*rxA*-*mango* or *rrnJ P1*-*mango* promoter DNA.

The -44 element, UP element, -35 element, -10 element and transcription products are highlighted in green, cyan, yellow, purple, and dark grey background, respectively. The *mango* sequence is colored in red with dark grey background.

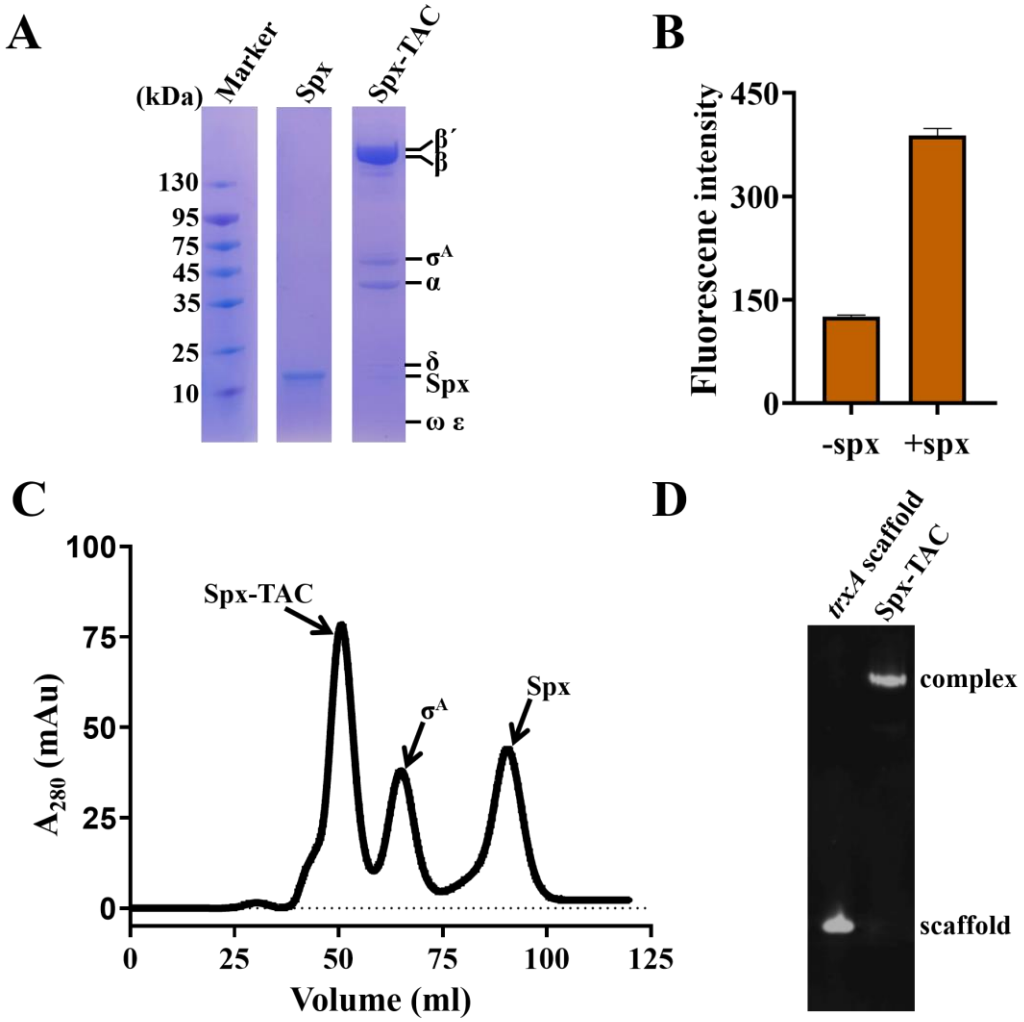

Figure S2. Purification and verification of *B. subtilis* Spx-TAC

(A) SDS-PAGE of the purified complex. 20 pmoles of complex was loaded.

(B) Relative transcription activity of *B. subtilis* RNAP-promoter open complex with or without Spx by using Mango-based transcription assay. Data for *in vitro* transcription assays are means of three technical replicates. Error bars represent mean ± SEM of n = 3 experiments.

(C) Chromatogram map of gel filtration.

(D) Native gel analysis of the purified complex. The gel was stained with 4S Red Plus Nucleic Acid Stain (Sangon Biotech, Inc.) according to the procedure of the manufacturer.

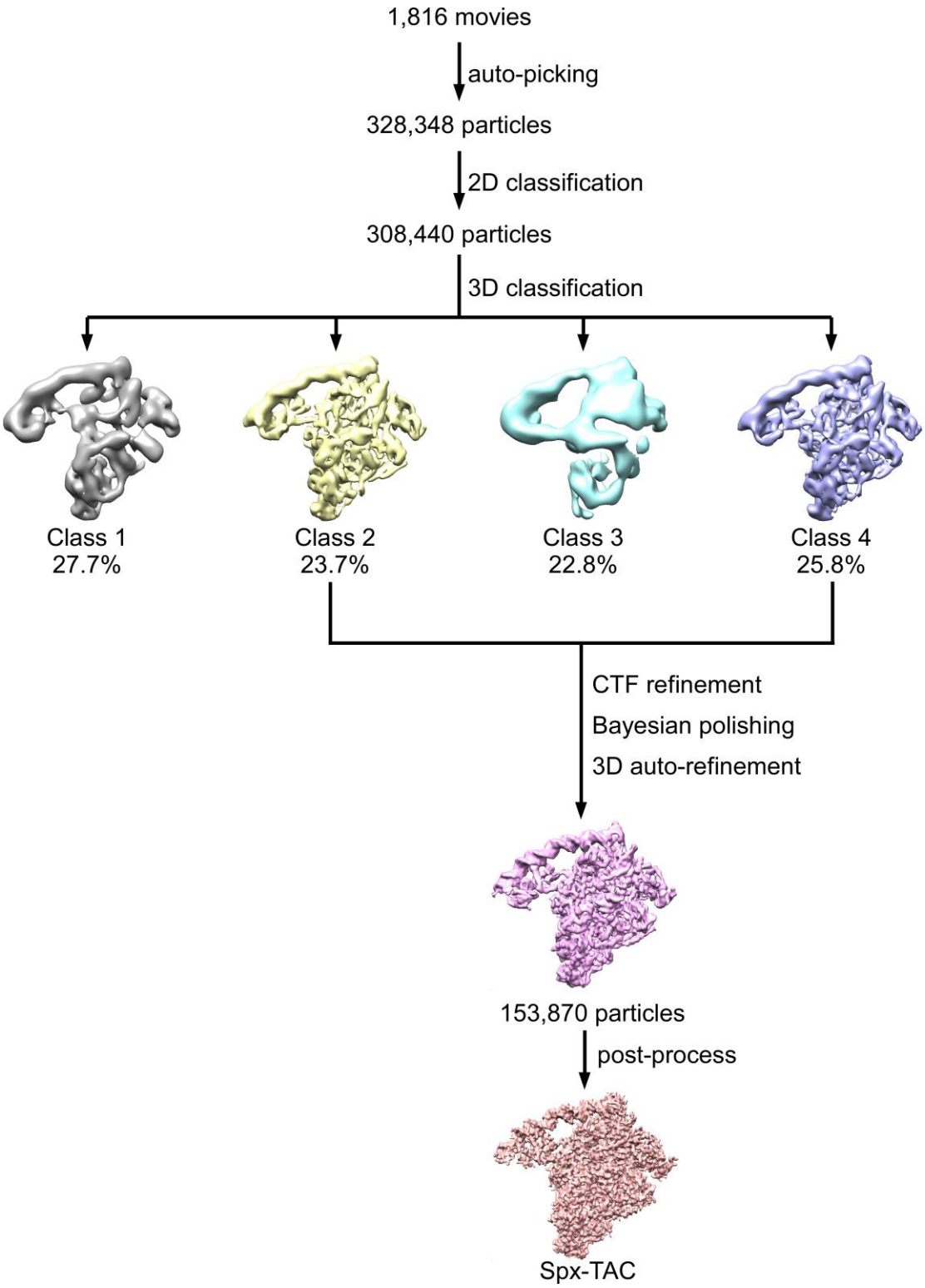

Figure S3. Data processing pipeline for the dataset of Spx-TAC.

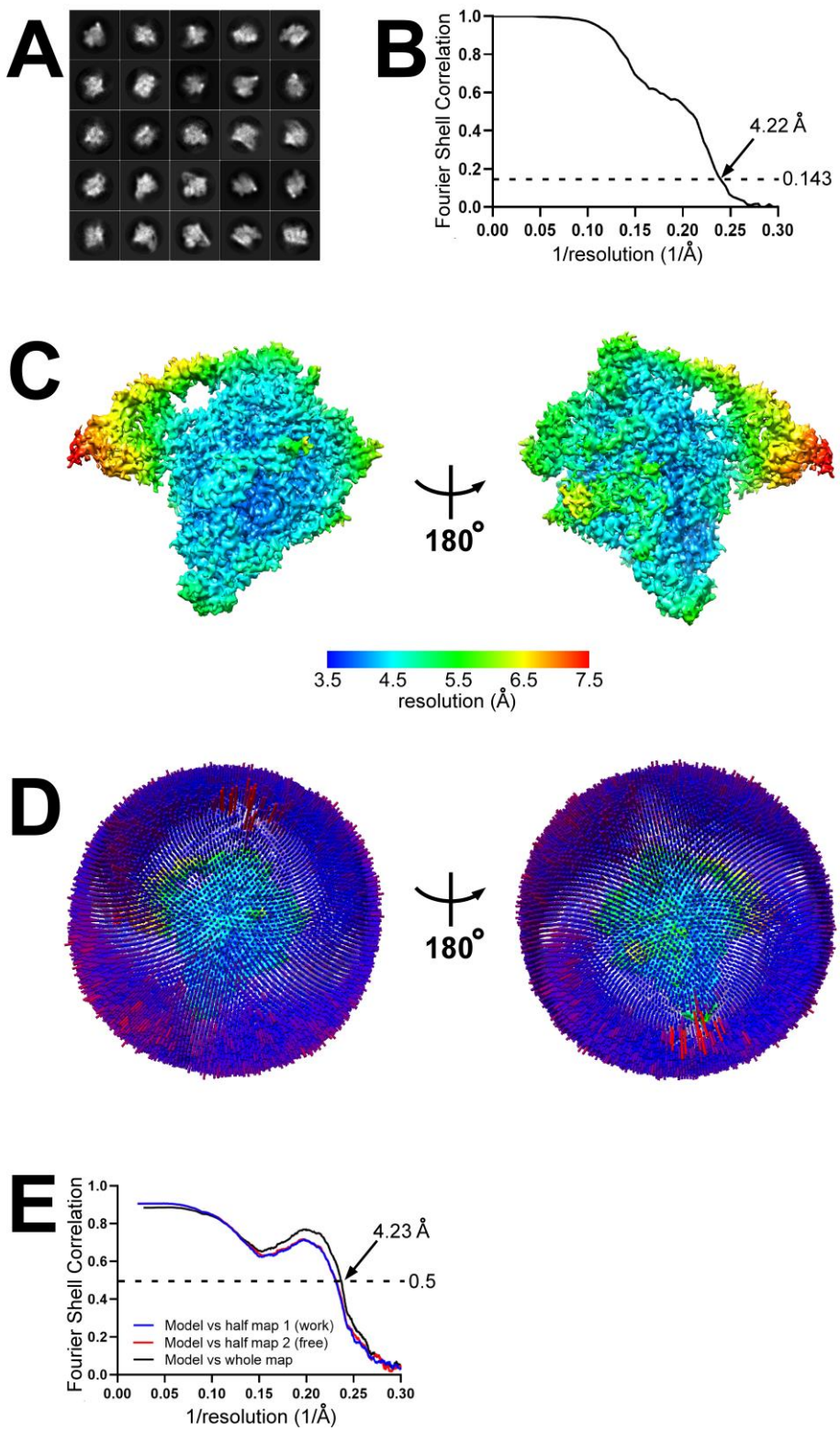

Figure. S4. Cryo-EM of *B. subtilis* Spx-TAC.

(A) Representative classes from 2D classification.

(B) Gold-standard FSC. The gold-standard FSC was calculated by comparing the two independently determined half-maps from RELION. The dashed line represents the 0.143 FSC cutoff, which indicates a nominal resolution of 4.22 Å.

(C) Cryo-EM density map colored by local resolution. Local resolution calculation was performed using blocres (1). View orientation as in **Figure 1B**.

(D) Angular distribution of particle projections. View orientations as in (C).

(E) FSC calculated between the model and the half map used for refinement (work), the other half map (free), and the full map.

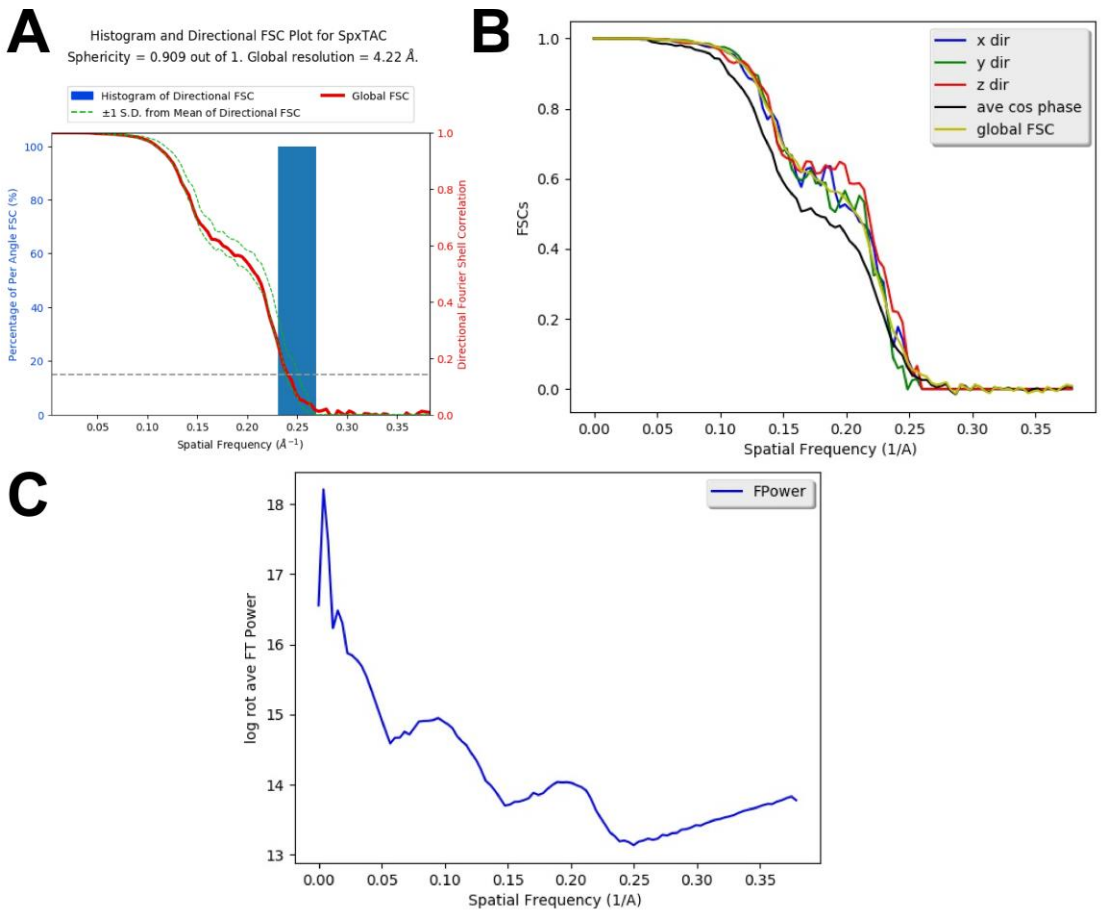

Figure. S5. The SPA quality assessment of *B. subtilis* Spx-TAC from remote 3DFSC processing server (https://3dfsc.salk.edu/) followed the procedures as (2). **(A)** Histogram and directional FSC Plot for *B. subtilis* Spx-TAC. **(B)** FSC plots for *B. subtilis* Spx-TAC. **(C)** FT power plot for *B. subtilis* Spx-TAC.

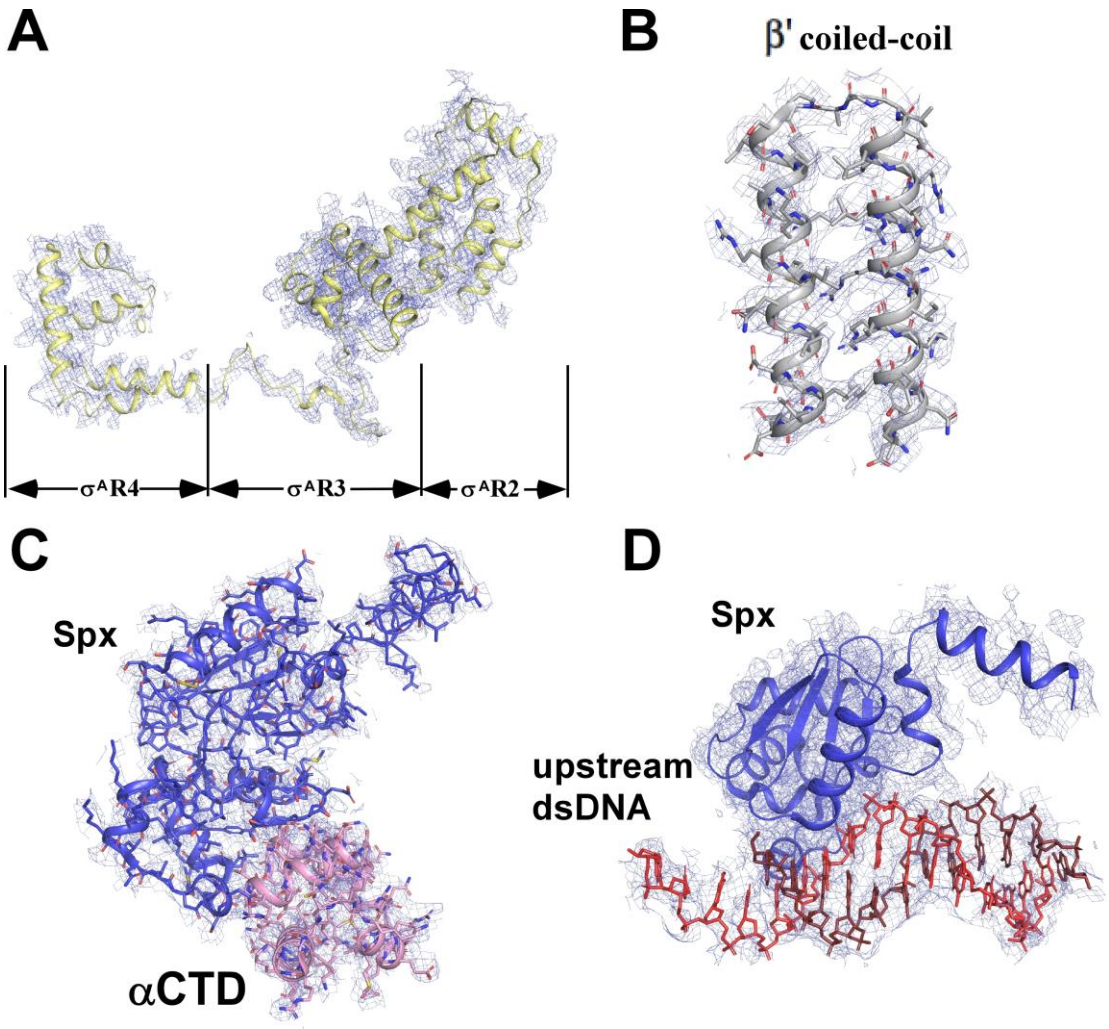

Figure S6. Representative cryo-EM densities of superimposed models in Spx-TAC.

(A) Cryo-EM density map (blue mesh) and the superimposed model (yellow cartoon) of σ^A. **(B)** Cryo-EM density map (blue mesh) and the superimposed model of β' coiled-coil. **(C)** Cryo-EM density map (blue mesh) and the superimposed model of Spx-RNAP αCTD subunit. **(D)** Cryo-EM density map (blue mesh) and the superimposed model of Spx-DNA. Other colors are shown as in **Figure 1**.

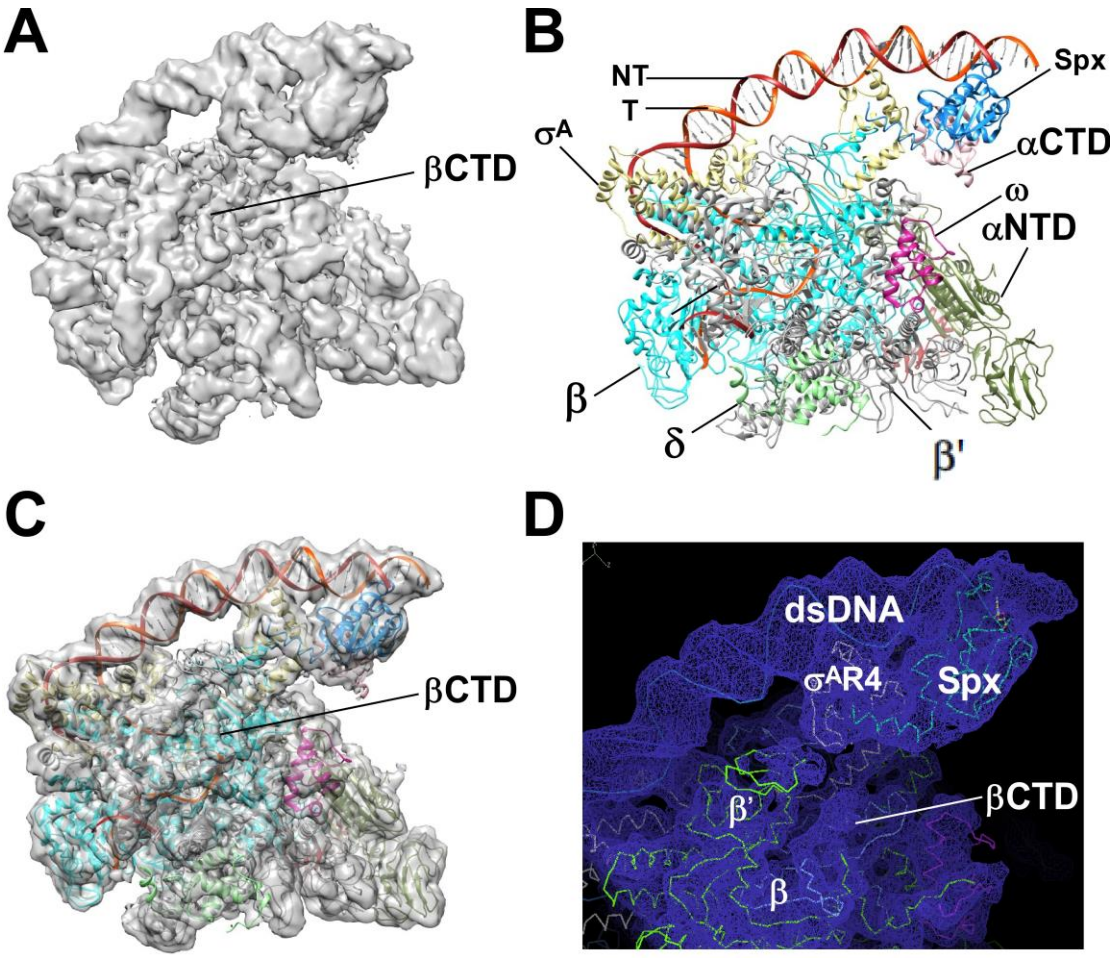

134

135 **Figure S7. Extra Cryo-EM density map for βCTD. (A-C)** Cryo-EM map and model for

136 Spx-TAC; **(D)** Extra Cryo-EM density map for βCTD is shown in coot. Other colors

137 are shown as in **Figure 1C**.

138

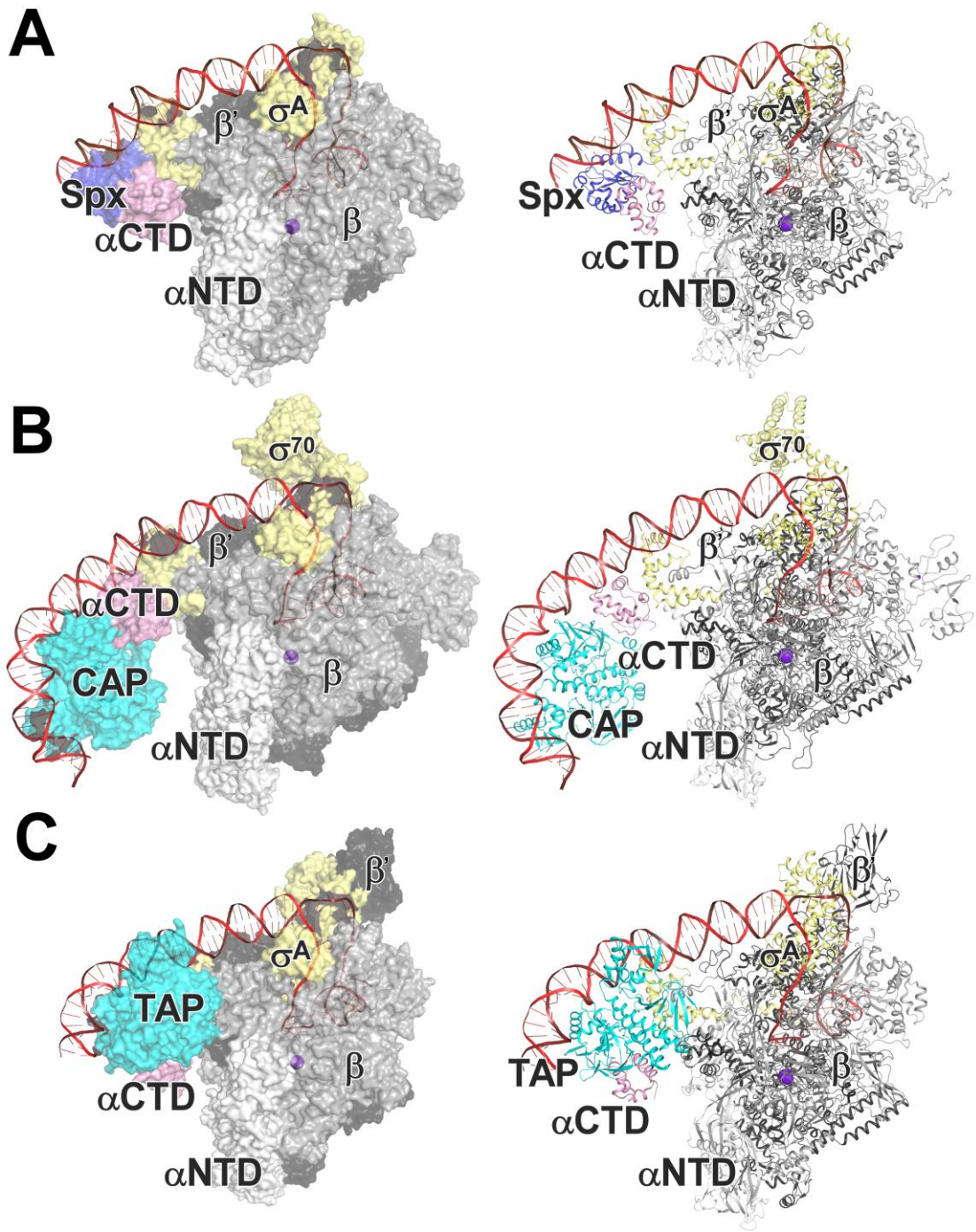

Figure S8. Comparisons of Spx-TAC, TAP-TAC and CAP-TAC.

(A-C) Spx-TAC, CAP-TAC and TAP-TAC (cartoon in left panel; surface in right panel). Cyan, CAP or TAP; blue, Spx; yellow, σ; white, pink, gray and dark gray, RNAP αNTD, αCTD, β, and β'.

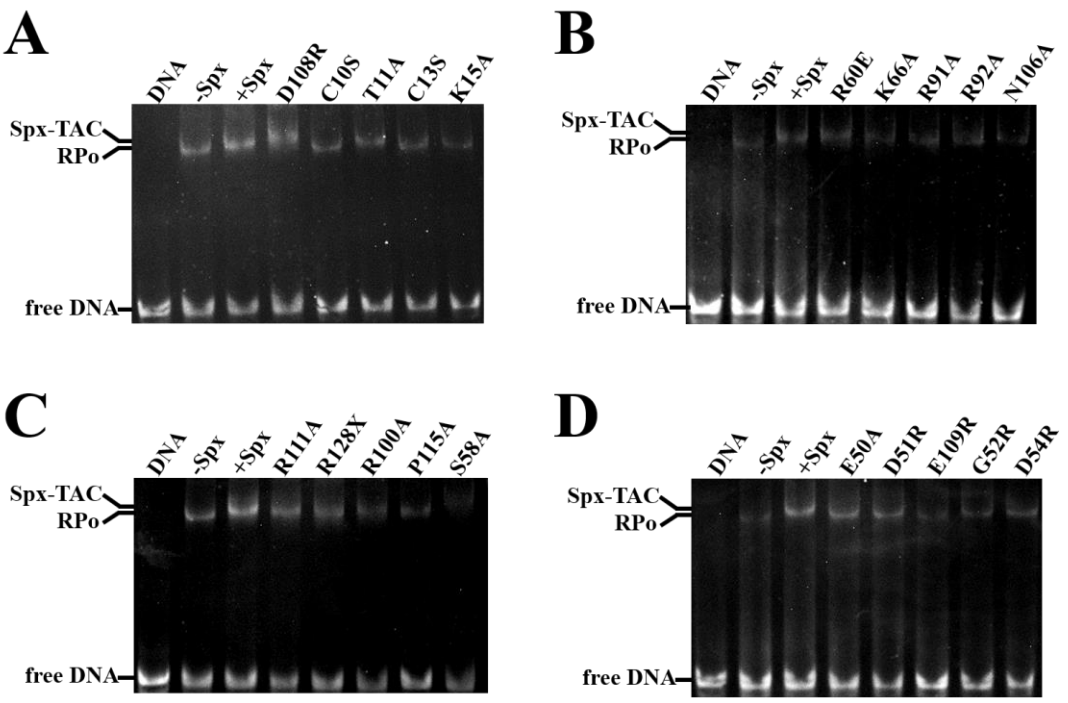

147

148 **Figure S9. Spx derivatives show defects on Spx-TAC formation.**

149 **(A)** Electrophoretic mobility shift assay for wild-type Spx and its mutants
150 (Spx-D108R, Spx-C10S, Spx-T11A, Spx-C13S and Spx-K15A). **(B)** Electrophoretic
151 mobility shift assay for wild-type Spx and its mutants (Spx-R60E, Spx-K66A,
152 Spx-R91A, Spx-R92A and Spx-N106A). **(C)** Electrophoretic mobility shift assay for
153 wild-type Spx and its mutants (Spx-R111A, Spx-R128X, Spx-R100A, Spx-P115A and
154 Spx-S58A). **(D)** Electrophoretic mobility shift assay for wild-type Spx and its mutants
155 (Spx-E50A, Spx-D51R, Spx-E109R, Spx-G52R and Spx-D54R). Reaction conditions
156 are described in detail in *Materials and Methods*. Bands of Spx-TAC, RPo and free
157 DNA (*trxA-mango* promoter DNA) are showed on the left, respectively.

158

159

160

161

162

163

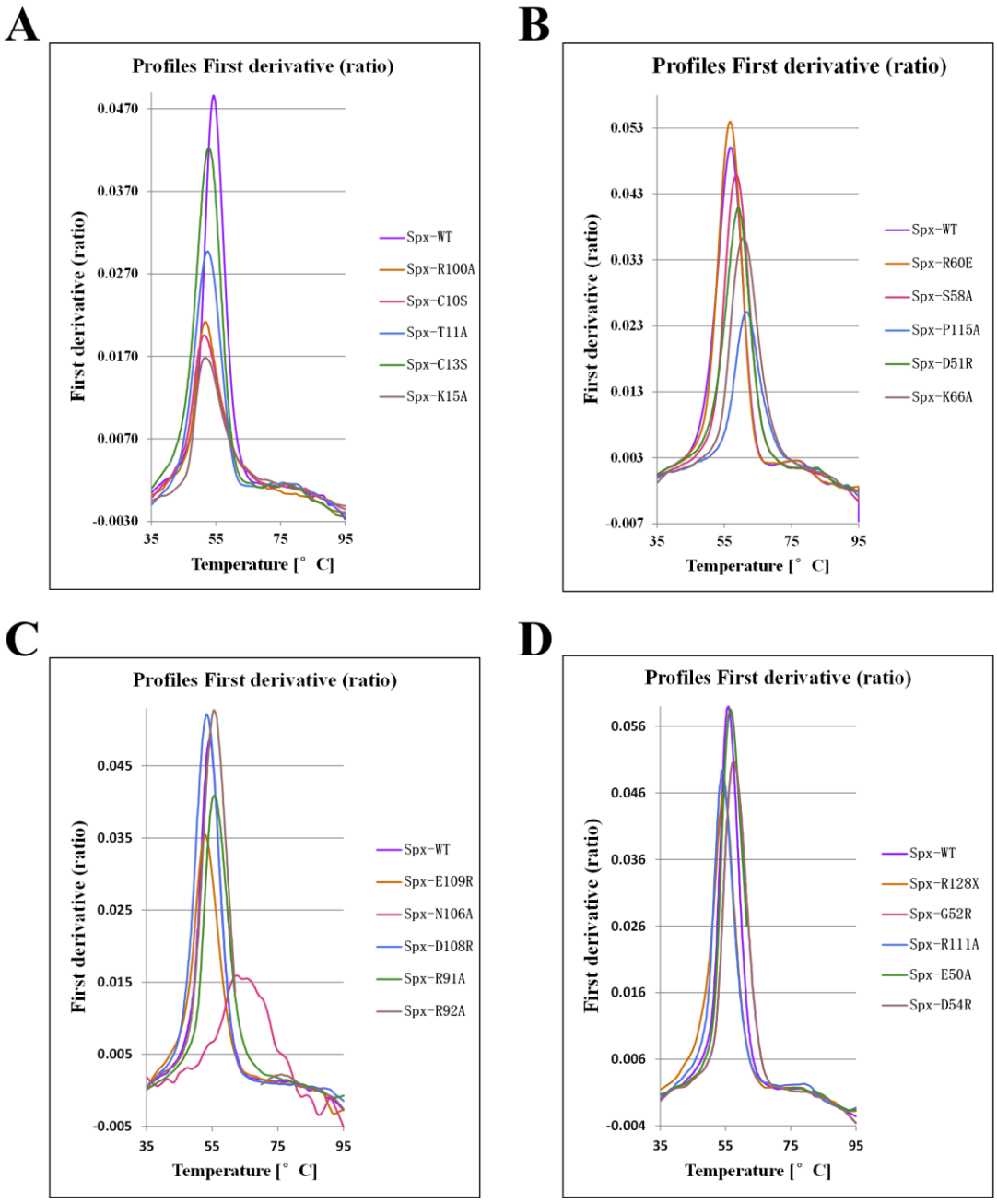

Figure S10 Thermal stability assays to detect the stabilities of wild-type Spx and its mutants and whether folded properly as wild-type Spx.

(A) Thermal stability assays for wild-type Spx and its mutants (Spx-R100A, Spx-C10S, Spx-T11A, Spx-C13S and Spx-K15A). **(B)** Thermal stability assays for wild-type Spx and its mutants (Spx-R60E, Spx-S58A, Spx-P115A, Spx-D51R and Spx-K66A). **(C)** Thermal stability assays for wild-type Spx and its mutants (Spx-E109R, Spx-N106A, Spx-D108R, Spx-R91A and Spx-R92A). **(D)** Thermal

stability assays for wild-type Spx and its mutants (Spx-R128X, Spx-G52R, Spx-R111A, Spx-E50A and Spx-D54R). If the thermostability curve of Spx mutants is similar to that of wild-type Spx, the stabilities of these mutants will be similar to wild-type Spx and it also means the mutant proteins folded properly.

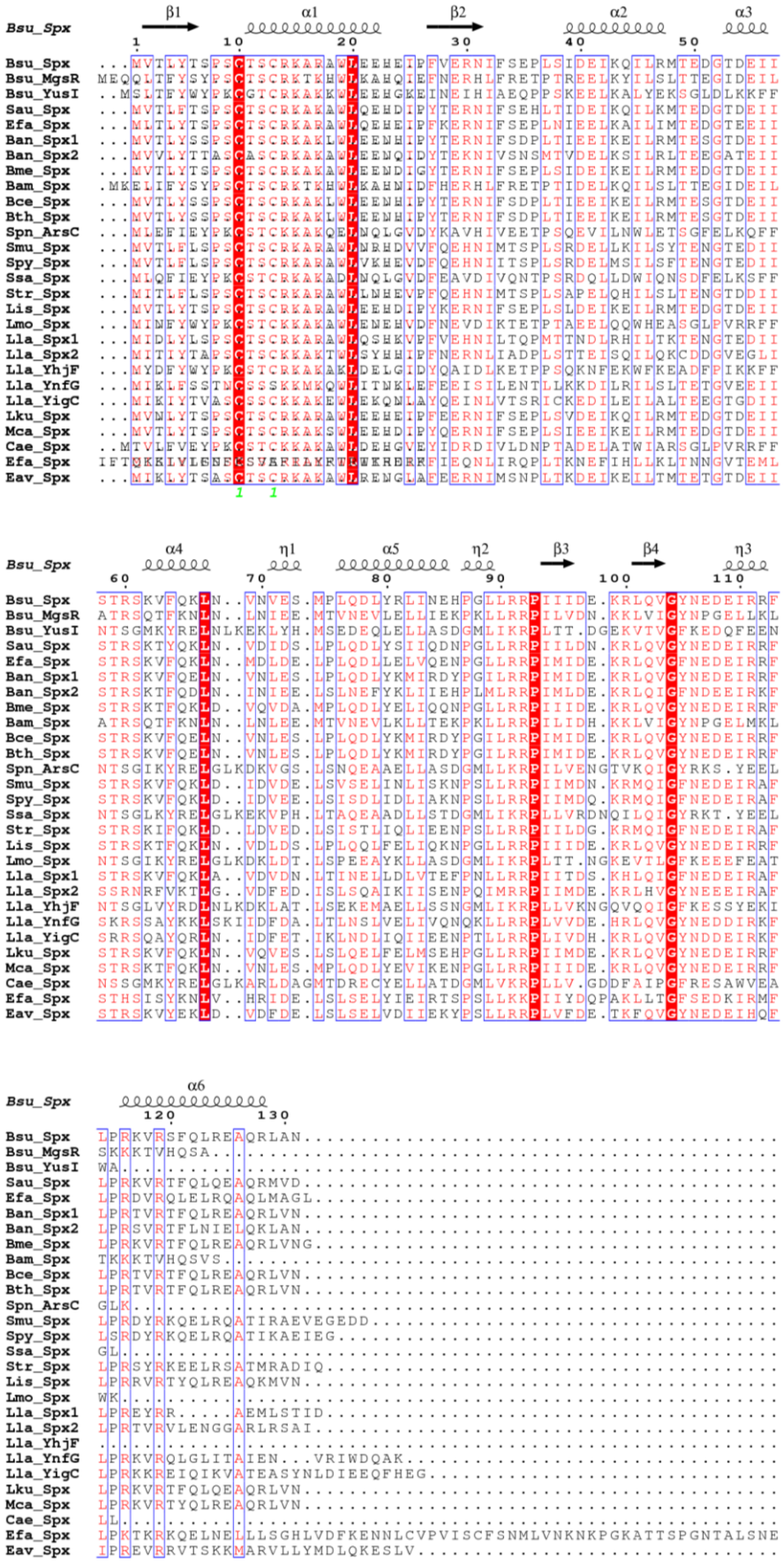

Figure S11 Protein sequence alignment of Spx from non-redundant 28

low-GC-content Gram-positive bacterial species. The sequences were extracted from UniProt Database by BLAST. The alignment was performed by Clustal Omega and the figure was prepared using ESPript 3.0 (3). The invariant residues among Spx from different low-GC-content Gram-positive bacteria are highlighted in red, and conserved amino acids are boxed.

Table S1. Primers and sequences used in this study.

Primer name	**Sequence (5′to 3′)**
*trxA-mango*_F1	cggctgtgatcaggaaaaaataatttgtaagcattaaaatagcgtgaacgaatgggag
*trxA-mango*_F2	atagcgtgaacgaatgggagatgctatactaaaaatcatcatttcacattggagg
*trxA-mango*_R1	ggcacgtacgaatataccacataccaatccttccttcgtacg
*trxA-mango*_R2	accaatccttccttcgtacgtgccgccattattgaattcctccaatgtgaaatgatg
*rrnJ P1-mango*_F1	tagggaaaggatgccgctctttttaaatcccttagtatttcttcaaaaaaactattgcac
*rrnJ P1-mango*_F2	cttcaaaaaaactattgcactattatttactaggtggtatattattattcgttgccgc
*rrnJ P1-mango*_R1	ggcacgtacgaatataccacataccaatccttccttcgtacgtgcc
*rrnJ P1-mango*_R2	tccttccttcgtacgtgcccgttatcgccttgtttagcggcaacgaataataatatacc
G52R sense	ctgcgtatgaccgaagatcgcaccgatgaaatc
G52R antisense	gatttcatcggtgcgatcttcggtcatacgcag
D54R sense	gaccgaagatggcacccgtgaaatcatctctacccg
D54R antisense	cgggtagagatgatttcacgggtgccatcttcggtc
C10S sense	gtacaccagcccgagcagcaccagctgcc
C10S antisense	ggcagctggtgctgctcgggctggtgtac
T11A sense	gcccgagctgcgccagctgccgt
T11A antisense	acggcagctggcgcagctcgggc
C13S sense	gagctgcaccagcagccgtaaagcgcgtg
C13S antisense	cacgcgctttacggctgctggtgcagctc
K15A sense	tgcaccagctgccgtgcagcgcgtgcgtggc
K15A antisense	acgcacgcgctgcacggcagctggtgcagc
S58A sense	gcaccgatgaaatcatcgctacccgtagcaaagt
S58A antisense	actttgctacgggtagcgatgatttcatcggtgc
R60E sense	caccgatgaaatcatctctaccgagagcaaagttttccagaaactg
R60E antisense	cagtttctggaaaactttgctctcggtagagatgatttcatcggtg
K66A sense	cgtagcaaagttttccaggagctgaacgttaacgttgaaagc
K66A antisense	gctttcaacgttaacgttcagctcctggaaaactttgctacg
R91A sense	catccgggtctgctggctcgtccgatcatcatc
R91A antisense	gatgatgatcggacgagccagcagacccggatg
R92A sense	catccgggtctgctgcgtgctccgatcatcatcgatg
R92A antisense	catggatgatgatcggagcacgcagcagacccggatg
N106A sense	tctgcaggttggttacgccgaagatgaaatccgtc
N106A antisense	acggatttcatcttcggcgtaaccaacctgcagac
D108R sense	gttggttacaacgaagctgaaatccgtcgtttcc
D108R antisense	gaaacgacggatttcagcttcgttgtaaccaacc
E50A sense	cctgcgtatgaccgcagatggcaccgatga
E50A antisense	catcggtgccatctgcggtcatacgcaggatc
D51R sense	tcctgcgtatgaccgaacgtggcaccgatgaaatc
D51R antisense	gatttcatcggtgccacgttcggtcatacgcagg
R100A sense	ccgatcatcatcgatgaaaaagctctgcaggttggttac
R100A antisense	accaacctgcagagctttttcatcgatgatgatcggac

E109R sense	tggttacaacgaagatgcaatccgtcgtttcctgc
E109R antisense	gcaggaaacgacggattgcatcttcgttgtaacca
R111A sense	acaacgaagatgaaatcgctcgtttcctgccgcgtaaag
R111A antisense	acgcggcaggaaacgagcgatttcatcttcgttgtaac
P115A sense	gaaatccgtcgtttcctggcgcgtaaagttcgtag
P115A antisense	ctacgaactttacgcgccaggaaacgacggatttc
R128X sense	ccagctgcgtgaagcgcagtagctggcgaactaaaagcttg
R128X antisense	caagcttttagttcgccagctactgcgcttcacgcagctgg
pET28a_F	caccaccaccaccaccactg
pET28a_R	gctgccgcgcggcaccag
Bs_α_F	gcctggtgccgcgcggcagcatgatcgagattgaaaaaccaaaa
Bs_α_R	cagtggtggtggtggtggtgtcaatcgtctttgcgaagtcc
Bs_σ^A_F	gcctggtgccgcgcggcagcatggctgataaacaaacccacg
Bs_σ^A_R	ctcagtggtggtggtggtggtgttattcaaggaaatctttcaaacg

Supplementary References

1. Cardone, G., Heymann, J.B. and Steven, A.C. (2013) One number does not fit all: mapping local variations in resolution in cryo-EM reconstructions. *J. Struct. Biol.*, **184**, 226-236.

2. Tan, Y.Z., Baldwin, P.R., Davis, J.H., Williamson, J.R., Potter, C.S., Carragher, B. and Lyumkis, D. (2017) Addressing preferred specimen orientation in single-particle cryo-EM through tilting. *Nature methods*., **14(8)**, p.793.

3. Robert, X. and Gouet, P. (2014) Deciphering key features in protein structures with the new ENDscript server. *Nucleic Acids Res.*, **42**, W320-W3244.